Available online at http://scik.org

J. Mater. Sci. Appl. 2013, 2013:5

ISSN 2051-5499

IMPROVING BARRIER PROPERTIES OF HDPE USING PVA AS CLAY MODIFIER

MARÍA CELESTE CARRERA[1,*], ELEONORA ERDMANN[2], JOSÉ MARÍA PASTOR[3] AND HUGO ALBERTO DESTÉFANIS[1]

[1]Instituto de Investigaciones para la Industria Química - INIQUI-CONICET, Consejo de Investigaciones- CIUNSa, Facultad de Ingeniería- UNSa, Avenida Bolivia 5150, 4400, Salta, Argentina

[2]Instituto Tecnológico de Buenos Aires-ITBA, Instituto de Investigaciones para la Industria Química INIQUI (UNSa-CONICET). Av. Eduardo Madero 399, C1106ACD, Buenos Aires, Argentina

[3]Dpto. Física de la Materia Condensada- Escuela de Ingenierías Industriales- Universidad de Valladolid, Centro de Investigación y Desarrollo en Transporte y Energía -CIDAUT, Paseo del Cauce 59, 47011, Valladolid, España

Abstract: In this work it was prepared nanocomposites of high density polyethylene (HDPE) with different loads of modified organoclay with polyvinylalcohol (PVA). Modified organoclay was obtained by "in situ" polymerization of vinyl acetate with an organoclay and the nanocomposites were prepared by melt blending. The structure and morphology of nanocomposites were studied by XRD, SEM and TEM. The heat stability was measured by TGA and DSC. The barrier properties were evaluated by testing of cyclohexane pervaporation and the surface properties were obtained by determination from the contact angle using three solvents at ambient atmosphere. TEM results showed the different types of nanocomposite structures that were obtained with clay layers in the polymer matrix depending on the load of clay incorporated into the polymer matrix. The permeation experiments confirmed that the barrier properties evaluated by cyclohexane pervaporation were

*Corresponding author

Received August 16, 2013

remarkably improved and increased in the thermal resistance for HDPE/ organoclay modified with PVA materials compared with pristine HDPE. Results from all studies showed that the addition of modified organoclay has changed the macroscopic properties of nanocomposites, as compared to that pure HDPE. This can be attributed to the different interaction of PVA with HDPE/filler.

Keywords: nanocomposites; pervaporation; HDPE; PVA.

1. Introduction

The preparation of polymer-clay nanocomposites by melt blending has been extensively reported [1-6]. This method involves the mixing of the layered silicate with the polymer and heating the mixture above its softening point. Under certain conditions, if the clay layer surfaces are sufficiently compatible with the polymer chains, the polymer can enter between the interlayer spaces, forming an intercalated/exfoliated structure [7-9]. The incorporation of small amounts (< 10 wt %) of clay showed a remarkable influence on the permeability and barrier properties of composite membranes [10].

The excellent barrier, with significant reduction of solvents and vapor permeability, is an attractive property and deeply explored for commercial applications. By improving the barrier properties of polymer/clay nanocomposites, potential applications for the material, are including the reinforcement of protective coating layers in civil plastic structures. In addition to the improvement of barrier properties, the addition of organoclays in polymers can also improve the thermal and mechanical properties of polymers [11, 12].

The dispersion/exfoliation of the clays in the polymer matrix and the chemical interaction between polymer and clay are the main factors to enhance the nanocomposite properties. For example, in the case of polyamides and some types of clay, the surface forces are very large due to hydrogen bond type interactions and the exfoliation is not a complex process. However, in the case of non-polar polymers like high density polyethylene (HDPE), there is poor interaction between hydrophilic clays and polymer and the adhesion between them is very weak, resulting in final materials

with mechanical and rheological properties well below the pristine polyethylene [13]. Several publications were reported associated with the study of improve interaction with hydrophobic polymers such as HDPE and clay organophilized, increasing polymer/clay affinity and the ability of forming exfoliated nanocomposites [7, 11, 13, 14 and 15]. However, preparation and properties of HDPE with organoclay modified with polyvinyl alcohol (PVA) have not been reported.

In this work, nanocomposites of HDPE and organoclay (exchanged with hexadecyltrimethylammonium-MMT_{HDTMA}) and MMT_{HDTMA} modified with PVA by in situ polymerization ($MMT_{HDTMA/PVA}$), were prepared by melt blending.

The aim is to investigate the influence of different filler content (0.6 wt%, 1 wt% and 2 wt %) of PVA-modified organoclay on the structure, barrier, and surface properties of nanocomposites with HDPE.

2. Materials and Experimental

A HDPE, 40055L from Polisur S. A with a melt flow index of 10g/10min (290 ℃, 21.6 kg) was chosen as the matrix.

Sodium montmorillonite (MMT) clay supplied by Minarmco (CEC = 70 meq (100 g)-1 and particle size <325 Mesh), was organically modified with a hexadecyltrimethylammonium bromide salt (MERCK) (HDTMA), following the modified technique of Yeh et al [16]. The organoclay was modified by in situ polymerization: the vinyl acetate monomer (vinyl acetate (VETEC, Brazil) was intercalated into the layers of MMT_{HDTMA} and followed by a free radical polymerization with benzoyl peroxide as a reaction initiator. The polyvinyl acetate/ MMT_{HDTMA} solution was saponified by alcoholysis with a NaOH solution to obtain polyvinyl alcohol modified organoclay ($MMT_{HDTMA/ PVA}$).

Mixing

HDPE/$MMT_{HDTMA/PVA}$ nanocomposites varying clay content (0.6 wt%, 1 wt% and 2 wt%) were prepared using a mixing chamber Rheomix 600, coupled to a HAAKE Rheocord 9000 torque rheometer with roller type rotors. The temperature and speed were 190 ℃ and 90 rpm respectively.

3. Characterization

Films of nanocomposites were prepared in a Carver Model 2086 hydraulic press, at a pressure of 27.6 MPa and 190 ℃ for 5 minutes.

X-ray diffraction (XRD) analyses were performed in a Rigaku Miniflex DRX 600 diffractometer, using nickel filtered CuKα radiation operating at 30 kV and 15 mA. The data were recorded at 2θ rate of 2 °min^{-1}.

Optical microscopy observations were made on a sample prepared by melting in a hot plate, using an Olympus microscope, model BX50 with polarized light.

The surface morphology of the obtained samples was observed by SEM in a JEOL JSM-6480 LV microscope with an accelerating voltage of 15kV, after gold coating.

In order to analyze the morphology of the nanocomposites, samples were observed by TEM in a Jeol JEM 2000FX microscope operating at 200 kV. The ultra thin sections of specimens were cut by cryo-ultramicrotome, RMC Power Tome XL, using a diamond knife. Thin sections of 60 nm were transferred into a copper grid.

4. Materials Properties

4.1 Thermal Properties

The thermal behaviour of the compounds was carried out using a TA Instrument TGA model Q500 from 30 ℃ to 700 ℃ with a heating rate of 10 ℃ min^{-1}, operating under N_2 flow of 60 ml min^{-1}. The melting point and fusion enthalpy were obtained by differential scanning calorimeter, DSC, model Q100, TA Instrument. Samples were heated from 20 ℃ to 200 ℃ at a rate of 10 ℃ min^{-1}, then cooled back to 20 ℃ and heated again at the same rate to 250 ℃ under N_2 atmosphere. The crystallinity data were obtained from the second heating run.

4.2 Properties physicochemical and of Transport

Solubility measurements of the membranes were carried out in test tubes with cyclohexane and submerged in a water bath to maintain the temperature at 50 ℃. Previously, the membranes were weighed and exposed for 97 hours to cyclohexane, they were then dried quickly and weighed at intervals of 24 hours to obtain the solubility/time curve.

Transport properties were performed in standard pervaporation equipment at 40 ℃ using the composite films of ~0.2 mm thickness. Vacuum at the downstream side was

maintained using a vacuum pump. Liquid nitrogen was used as cooler in order to collect all permeated vapors. A peristaltic pump was used to make circulate the solvent used (cyclohexane). The permeability was obtained from a gravimetric method.

4.3 Properties of Surfaces

Surface properties were obtained from measurements of contact angles, which were measured in digital standard-hart Ramé Model 200 goniometer, using three solvents: deionized water, anhydrous ethylene glycol (purity ≥ 99.75%) and diiodomethane, reagentplus (99% purity) supplied by Sigma-Aldrich at ambient atmosphere. All the contact angle values presented in this paper were averaged over five different positions.

5. Results and discussion

5.1 Morphology and Structure

XRD is a technique used to identify intercalated structures of nanocomposites. The Figure 1 shows XRD of unmodified organoclay (MMT_{HDTMA}) and the modified clay mixed with HDPE. The peak at low angle of 4.6 degrees in Figure 1 corresponds to the basal reflection (001) of the organoclay (MMT_{HDTMA}), for the HDPE/$MMT_{HDTMA/PVA}$ materials, with load of 0.6 wt% and 1 wt%, were observed peaks $2\theta = 3.76$ degrees indicating a intercalated structure, however when the load was higher, 2 wt%, no peaks were observed on the diffraction curves between 2-5 degrees, either because of a much too large spacing between the layers (i.e. exceeding 8 nm in the case of ordered exfoliated structure) or because the nanocomposite does not present ordering anymore [7].

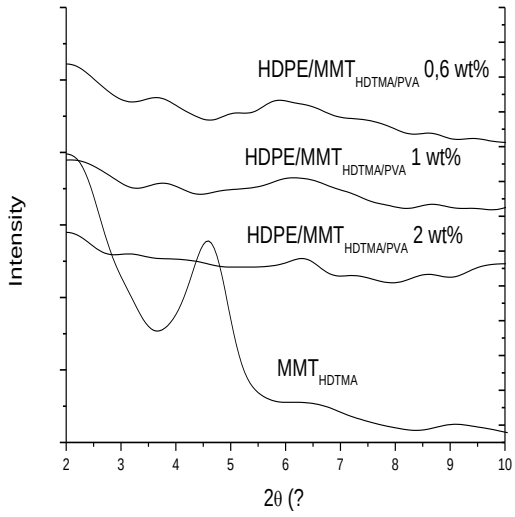

Figure 1. X-Ray diffraction curves of (a) HDPE, HDPE/$MMT_{HDTMA/PVA}$ with clay content (b) 0.6 wt%, (c) 1 wt%, and (d) 2 wt% and (e) MMT_{HDTMA}.

In this case, transmission electronic spectroscopy (TEM) was used to characterize the nanocomposite morphology [5]. Figure 2 shows the TEM micrographs with completely different structures corresponding to two different loads of $MMT_{HDTMA/PVA}$ in the polyethylene polymer matrix. For a load of 0.6 wt% (Figure 2a), the presence of two types of structures was observed, some larger tactoids could also be identified, and others in which the clay layers were intercalated in the polymeric matrix, this result was consistent with the micrographs obtained by XRD. However when a clay load of 2% was added, a mixed structure intercalated and or exfoliated was observed, Figure 2 (b). Thus, were considered XRD and TEM complementary techniques to each other for the characterization of materials such as polymer/clay nanocomposites and to confirm the type of structure formed therein [7].

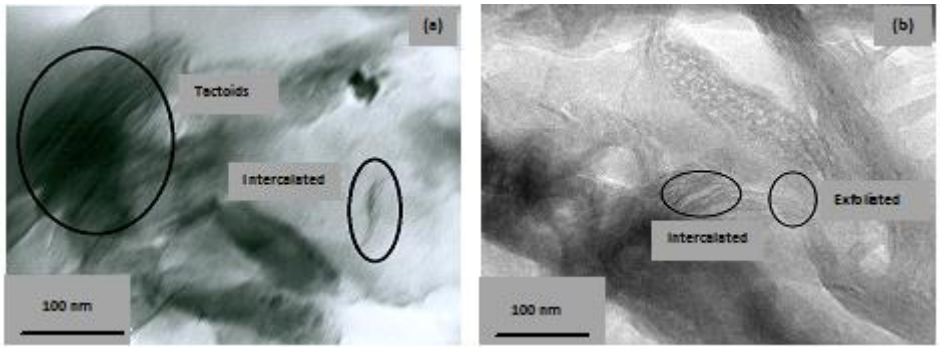

Figure 2. TEM images of HDPE/$MMT_{HDTMA/PVA}$ containing (a) 0.6 wt% and (b) 2 wt% of clay.

SEM micrograph of the Figure 3 (a) presents the typical morphology of a binary mixture of HDPE and PVA which are incompatible polymers. It shows large PVA particles with poor interfacial adhesion and dispersion in the polyethylene matrix. The morphology improves when the load organoclay in the polymer matrix was increased, especially when were high the loads, Figure 3 (c), indicating that a much more homogeneous material and a better dispersion had been obtained. These results were consistent with those obtained by TEM.

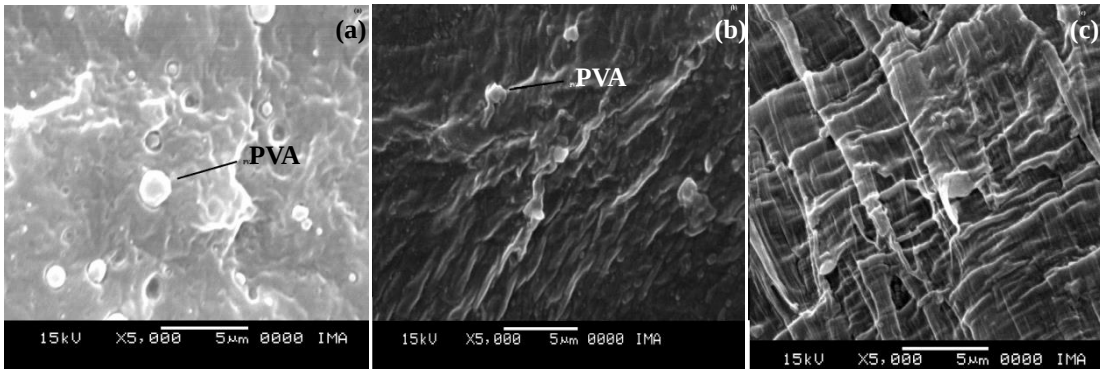

Figure 3. SEM images of HDPE/$MMT_{HDTMA/PVA}$ containing:

(a) 0.6 wt%, (b) 1 wt% and (c) 2 wt% of clay.

5.2 Thermal Properties

Figure 4 shows the weight and the derivate of weight with respect to time of HDPE and composite versus temperature, in general terms, the thermal stability of the HDPE composite materials obtained by TGA is enhanced with respect the pristine HDPE when the filler load increases. The presence of $MMT_{HDTMA/PVA}$ changes the profile of polyethylene DTGA shows the decomposition of PVA (dehydration: 200 ℃- 400 ℃) and decomposition of the ammonium salt (HDTMA) of the organically modify clay in the HDPE matrix in the same temperature range (Figure 4).

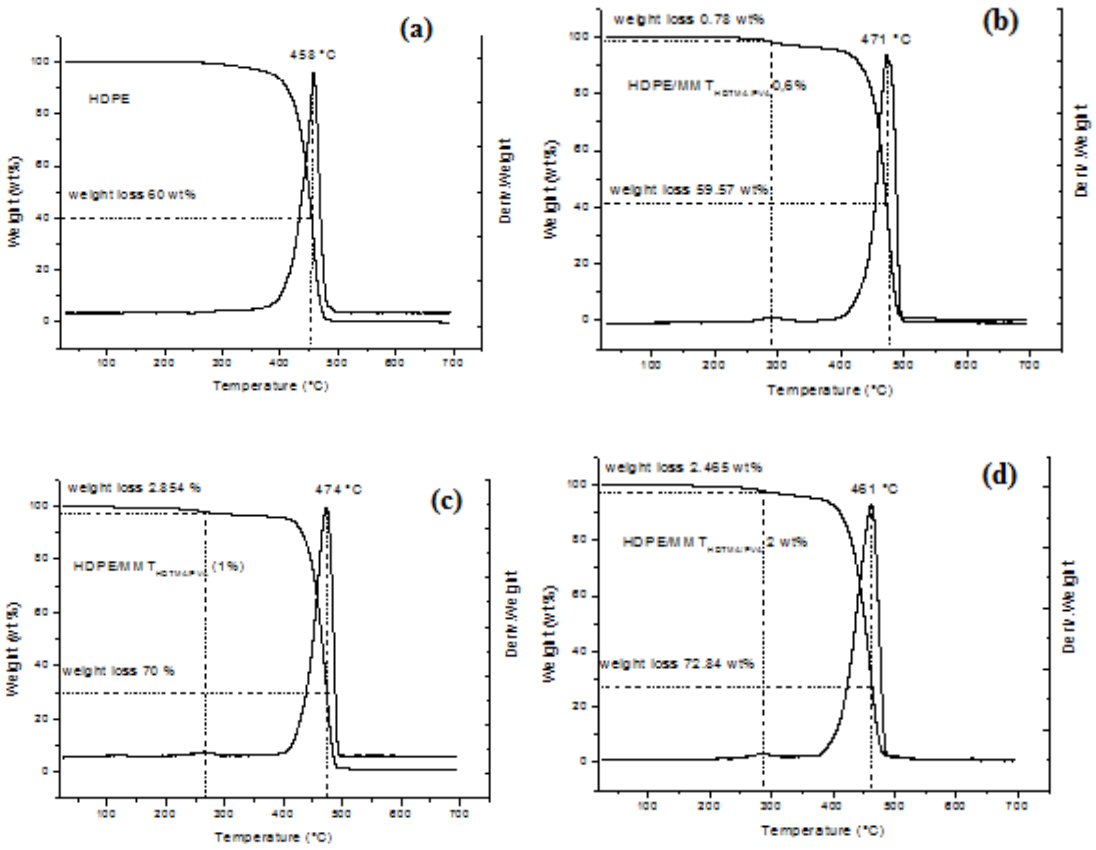

Figure 4. TG and DTG curves of (a) HDPE and HDPE/$MMT_{HDTMA/PVA}$ containing (b) 0.6 wt%, (c) 1 wt% and (d) 2 wt% of the clay.

Table 1 shows the weight loss to the maxim temperature of decomposition and materials with higher thermal resistance were those with lower clay load (0.6wt % and 1wt %).

Table. 1. Maxim temperature of weight loss and weight loss of HDPE and PVA in composites.

Sample	$T_{max.}$ weight loss (℃)	PVA weight loss (wt %)	HDPE weight loss (wt %)
HDPE	458	-	60
HDPE/$MMT_{HDTMA/PVA}$ 0.6 wt%	471	0.78	58.79
HDPE/$MMT_{HDTMA/PVA}$ 1 wt%	474	2.854	70
HDPE/$MMT_{HDTMA/PVA}$ 2 wt%	461	2.465	72.84

DSC traces of HDPE and HDPE/$MMT_{HDTMA/PVA}$ nanocomposites are shown in Figure 5. The melting point (T_m) of the nanocomposites did not change with regard to the T_m of pristine HDPE.

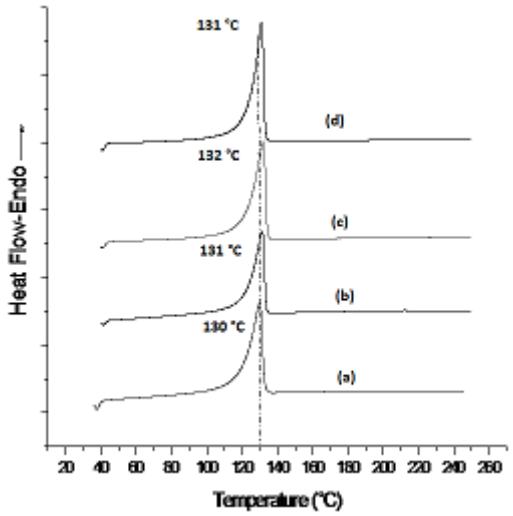

Figure 5. DSC curves of: (a) HDPE and HDPE/$MMT_{HDTMA/PVA}$ containing: (b) 0.6 wt%, (c) 1 wt% and (d) 2 wt% of the clay.

The polymers to be semi-crystalline materials are heterogeneous systems, where ordered crystalline regions are surrounded by amorphous regions, so the properties are influenced by the degree of crystallinity and the size and shape of the crystals. The crystallinity values were calculated using the total enthalpy method [17] from the equation (1), using melting enthalpy values (Table 2) of each material (ΔH_m), obtained from the area under the curve of heat versus temperature, Figure 5.

$$\chi_C = \frac{\Delta H_m}{\Delta H_m^0} \qquad (1)$$

Where: ΔH_m^0: crystalline fusion enthalpy to 100% crystalline polyethylene (ΔH_m^0 = 288 J g^{-1}) [18].

ΔH_m: material fusion enthalpy.

The results in Table 2 show that the crystallinity degree of the nanocomposites decreases regard to pure polymer favouring the increase of the amorphous phase in the polymer [19]. This decrease may be attributed to higher interfacial area and adhesion between the HDPE matrix and modified organoclay, which would act to reduce the mobility of HDPE crystallines chain segments [13].

Table. 2. Fusion enthalpy and crystalline degree of the materials.

Sample	ΔH_m (J g^{-1})	χ_C (%)
HDPE	156.1	54.2
HDPE/$MMT_{HDTMA/PVA}$ 0.6 wt%	131.8	50
HDPE/$MMT_{HDTMA/PVA}$ 1 wt%	140.7	49
HDPE/$MMT_{HDTMA/PVA}$ 2 wt%	142.0	49.3

5.3 Properties physicochemical and of Transport

Pervaporation results at 40 ℃ were used to obtain the permeability factor (P); these values are shown in Table 3. Lower P with respect to pristine HDPE was obtained for the composite membranes (around 90%). When the organoclay-modified PVA was incorporated as filler, the barrier properties with respect to hydrocarbons were dramatically improved as compared to pristine polymer. This was attributed to the clay which acted as a barrier to the transport of matter, however the factor that most affects the permeation is the presence of PVA in the clay, a polar molecule, able to interact through hydrogen bridge bond formation, causes decreased permeability by the low affinity for permeant solvent (cyclohexane). In the work of Erdmann et al. [20] were reported values cyclohexane permeation in HDPE /clay modified with molecules of different polarity, but with no or little ability to hydrogen bond formation links, and showed an effect on barrier properties far below those achieved with PVA.

Table 3. Permeability factor (P) and P decrease.

Sample	P[g.mm.h^{-1}.m^{-2}] (40 ℃)	P decrease [%]
HDPE	17.76	-
HDPE/$MMT_{HDTMA/PVA}$ 0.6 wt%	0.59	97
HDPE/$MMT_{HDTMA/PVA}$ 1 wt%	1.03	94
HDPE/$MMT_{HDTMA/PVA}$ 2 wt%	0.58	97

Vapor permeation in a membrane is a process in which molecules are initially adsorbed on the membrane surface and then diffuse through the membrane. During adsorption, the vapor molecules are placed in the holes of the polymer (free volume) that are created by Brownian movements of the chains or by thermal perturbations. The diffusion process occurs by jumps through neighbouring holes. Thus, this process depends on the number and size of these (static free volume) and the frequency of jumps (dynamic free volume). The static free volume is independent of the thermal motions of the macromolecules and is related to the solubility of vapor, while the dynamic free volume originates from the segmental motions of polymer chains and is related to the diffusivity of the vapor. Thus, the diffusion coefficient is a kinetic factor that reflects the mobility of vapor molecules in the polymer phase, while the solubility coefficient (*S*) is a thermodynamic factor, related to the interactions between the polymer and vapor molecules.

The solubility coefficient (*S*) was calculated using equation (2):

$$S(\%) = \left(\frac{W_i - W_s}{W_s}\right).10 \qquad (2)$$

Where:

W_i: mass of the swollen membrane.

W_s: mass of dry membrane.

Table 4 shows the percentages of solubility at 40 °C and 50 °C. Comparing polymer blends with different clay loadings can be seen that adding 2 wt% of clay, the solubility decreases with regard to pure polyethylene approximately 4%, which was favourable in reducing cyclohexane permeability, this is verified with pervaporation results (Table 3), having accounted for the dependence of the permeability factor to the solubility given in equation (3). In nanocomposites the solubility decreases with respect to a pure polymer, due to the reduction in the volume of polymer matrix as the decrease in diffusion due to the tortuous path, caused by the clay sheets to the diffused molecules [21].

Also verified is that the solubility as a function of temperature follows the Arrhenius law and that increasing the temperature the percentage solubility of the membranes

also increased by about an order of magnitude over the lower temperature.

Table 4. Solubility in cyclohexane to 40 ℃ and 50 ℃.

Sample	S (wt %)	
	40 ℃	50 ℃
HDPE	8.48	9.37
HDPE/$MMT_{HDTMA/PVA}$ (0.6 wt%)	8.48	9.24
HDPE/$MMT_{HDTMA/PVA}$ (1 wt%)	8.56	9.50
HDPE/$MMT_{HDTMA/PVA}$ (2 wt%)	8.17	9.17

The experiments of adsorption/desorption, served to estimate the solubility and the diffusion coefficient, which allow calculation of permeability using the equation (3):

$$P = D.S \qquad (3)$$

Where: *P*: permeability coefficient, *D*: diffusion coefficient and *S*: adsorption coefficient or solubility.

The fractional mass adsorption is presented as a function of time. Assuming a flat membrane of thickness "*d*" and the uniform concentration of cyclohexane in the membrane, one of the possible solutions of equation (4) is the equation (5) [22].

$$D\nabla^2 c(r,t) = \frac{\partial c(r,t)}{\partial t} \qquad (4)$$

$$\frac{M_t}{M_\infty} = 8.\sqrt{\frac{D.t}{d^2}}\left[\frac{1}{\sqrt{\pi}} + 2.\sum_{m=0}^{\infty}(-1)^m i\,e\,r\,f\,c\left(\frac{m.d}{4.(D.t)^{1/2}}\right)\right] \qquad (5)$$

Where M_t and M_∞ are the mass adsorbed at time t and infinite time, respectively. Also ierfc is the error integral function.

Equation (5) converges rapidly for short times and is as follows:

$$\frac{M_t}{M_\infty} = \frac{8}{\pi^{1/2}}.\left(\frac{D.t}{d^2}\right)^{1/2} \qquad (6)$$

Plotting M_t / M_∞ and $t^{1/2}/d$ (Figure 6) results in a straight line until $t^{1/2}$, the average lifetime when $M_t/ M_\infty = 1/2$. The diffusion coefficient is calculated from the slope of that line [23].

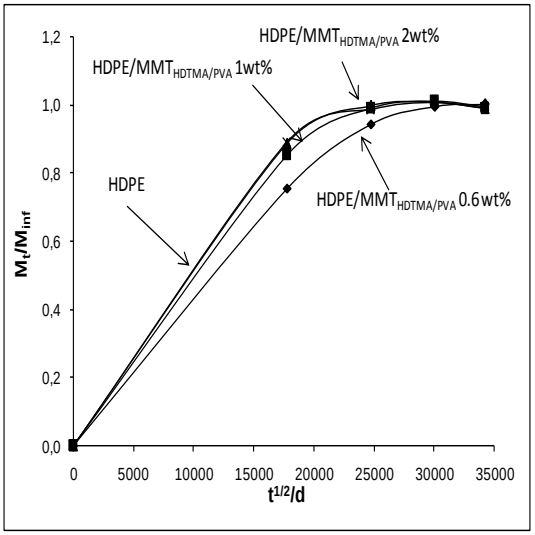

Figure 6. Diagram of experimental measurements of adsorption/desorption: HDPE / $MMT_{HDTMA / PVA}$ with different clay loadings (0 wt%, 0.6 wt%, 1 wt% and 2 wt %).

Table 5 shows that decreases the diffusion coefficient (*D*), reaching a minimum to a clay loading of 0.6 wt% compared to HDPE, but when the load increases, the coefficient (*D*) begins to rise until it reaches the value corresponding to pure polyethylene.

Table 5. Diffusivity coefficient for HDPE/$MMT_{HDTMA/PVA}$ materials with different clay loadings (0%, 0.6 wt%, 1 wt% and 2 wt%).

Sample	D.10^{10} (cm^2s^{-1})
HDPE	1.24
HDPE/$MMT_{HDTMA/PVA}$ (0.6 wt%)	0.887
HDPE/$MMT_{HDTMA/PVA}$ (1 wt%)	1.13
HDPE/$MMT_{HDTMA/PVA}$ (2 wt%)	1.22

5.4 Properties of Surfaces

From contact angles were obtained both adhesion work and surface tension.

To calculate the adhesion work, Young and Dupree's Equation 7 was taken into account. The surface tension can be obtained according to Figure 7.

$$W_a = \gamma_1 + \gamma_2 - \gamma_{12} = \gamma_1 + \gamma_1 \cos\theta = \gamma_1 (1 + \cos\theta) \qquad (7)$$

W_a: work of adhesion

γ_1: surface tension (air/substance)

γ_2: surface tension (air/film)

γ_{12}: surface tension (substance/film)

θ: contact angle

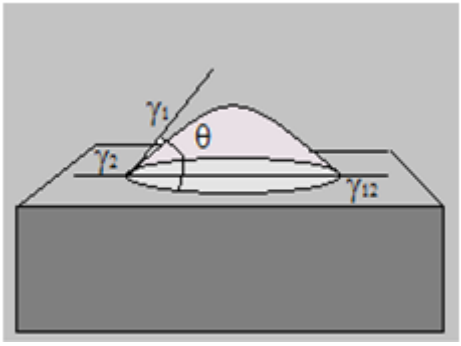

Figure 7. Contact angle and superficial tensions.

The materials surface energy was obtained from the method proposed by Rabel [24]. DROP image Surface Energy (Multi Liquids) tool of goniometer was used for this calculation.

Figure 8 shows the decrease in surface tension when clay loads different were incorporated into the polymer matrix.

This results, showing the same tendency as the permeability factor (P) obtained by pervaporation, which was consistent, because when it comes to establishing a barrier to the hydrocarbon permeability, the low affinity between of PVA (clay) /hydrocarbon results in a decline of surface tension.

This correlation between permeability and surface tension was associated with the pervaporation mechanism that involves three stages. The first: interaction between the liquid and the surface of the membrane, governed by the nature of the solid (membrane) and liquid (hydrocarbon). The more hydrophilic surface of the nanocomposites repels hydrocarbon molecules, becoming the controlling step and most important of the pervaporation process, as it was the stage of contact with the hydrocarbon membrane which is then countered with what is proven with the surface phenomenon associated with this stage which reduces the surface tension reflected in Figure 8.

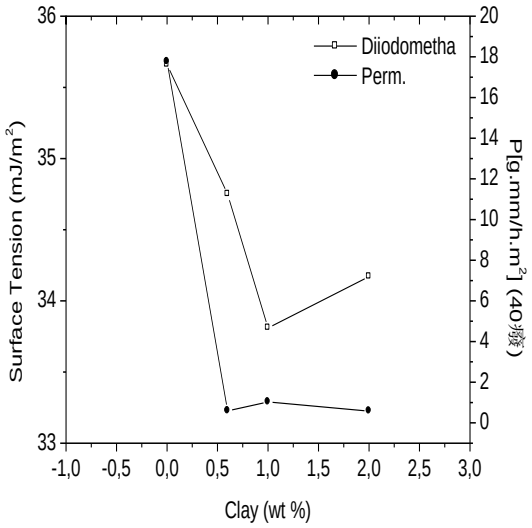

Figure 8. Correlation of surface tension and permeability vs. clay content.

The experimental results allow formulating a possible mechanism of interaction between the PVA-modified organoclay and HDPE polymer matrix. Different types of interactions are present in this polymer system and considering the chemical nature of the types involved at different stages, the mechanism shown in Figure 9 was proposed.

Using the above experimental results a possible mechanism can be formulated of interaction between the organoclay modified with PVA and the polymer matrix of HDPE in response to the different interactions that can be supposed present and the chemical nature of the species involved, at different stages of the proposed mechanism in Figure 9. There are hydrogen bond type interactions outside of MMT_{HDTMA} layers between the silicate oxygen and the PVA hydroxyl groups. The same type of interaction occurs between the hydroxyl groups in the interior and at the edges of the clay layers.

In the 2^{nd} stage of the process of nanocomposites preparation, during the melting of polyethylene in presence of the PVA-modified organoclay, HDPE interacts with the aliphatic moieties of PVA outside the clay layers and aliphatic chains on the inside of the clay can bind to the hydrocarbon chains of polyethylene, ie both inside and out the clay layers are dispersive type interactions, finally reaching the breaking of the ordered structure of the clay galleries to achieve a homogenous dispersion of the same

in the HDPE polymer matrix to form a nanocomposites as shown in the 3rd stage of Figure 9. PVA chains surrounding clay sheets retain polar hydroxyl groups that are responsible for conferring a hydrophilic polymer surface, repelling the hydrocarbon molecules and decreasing its permeability.

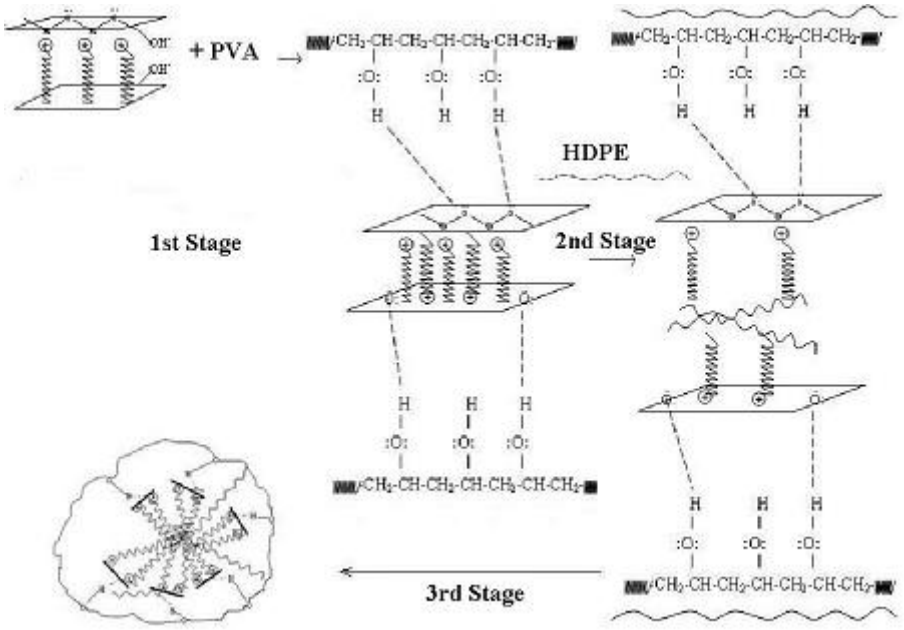

Figure 9. Proposed interaction mechanism between HDPE and $MMT_{HDTMA/PVA}$.

Acknowledgement: Consejo Nacional de Investigación Científica y tecnológica (CONICET), Argentina.

Financial support of CAPES/SECyT is gratefully acknowledged.

EADIC, ERASMUS MUNDUS EXTERNAL COOPERATION WINDOWS LOT 16. Sandwich PhD Scholarship in Universidad de Valladolid, Escuela de Ingenierías Industriales, España.

Conflict of Interests

The author declares that there is no conflict of interests.

REFERENCES

[1] H. R Dennis, D. L Hunter, D. Chang,S. Kim, J. L White, J. W Cho, D. R Paul, Polymer. 42 (2001), 9513.

[2] J. W Gilman, A. B Morgan, E. P Giannelis, M. Wuthenow, E. Manias, BCC conference on Flame Retardancy. 1 (1999).

[3] P. G Nahin, P. S Backlund, Organoclay Polyolefin Compositions. (1963). US Patent 3084117. Union Oil Co.

[4] R. A Vaia, H. Ishii, E. P Giannelis, Chemistry of Materials. 5 (1993), 1694.

[5] R. A Vaia, K. D Jant, E. J Kramer, E. P Giannelis, Chemistry of Materials. 8 (1996), 2628.

[6] R. A Vaia, E. P Giannelis, Macromolecules. 30 (1997), 7990.

[7] M. Alexandre, P. Dubois, Materials Science and Engineering. 28 (2000), 1.

[8] S. Pavlidoua, C. D Papaspyrides, Progress in Polymer Science. 33 (2008), 1119.

[9] P. C LeBaron, Z. Wang, T. J Pinnavaia, Applied Clay Science. 15 (1999), 11.

[10] J. K Kim, C. Hu, R. S. C Woo, M. L Sham, Composites Science and Technology. 65 (2005), 805.

[11] S. Choi, K. M Lee, C. D Han, Macromolecules. 37 (2004), 7649.

[12] D. Garc á-L ópez, I. Gobernado-Mitre, J. F Fern ández, J. C Merino, J. M Pastor, Polymer. 46 (2005), 2758.

[13] T. G Gopakumar, J. A Lee, M. Kontopoulou, J. S Parent, Polymer. 43 (2002), 5483.

[14] K. Chrissopoulou, I. Altintzi, S. H Anastasiadis, E. P Giannelis, M. Pitsikalis, N. Hadjichristidis, N. Theophilou, Polymer. 46 (2005), 12440.

[15] G. Gorrasi, M. Tortora, V. Vittoria, E. Pollet, B. Lepoittevin, M. Alexandre, P. Dubois, Polymer. 44 (2003), 2271.

[16] J. M Yeh, H. Y Huang, C. L Chen, W. F Su, Y. H Yu, Surface & Coating Technology. 200 (2006), 2753.

[17] H. A Khonakdar, J. Morshedian, U. Wagenknecht, S. H Jafari, Polymer. 44 (2003), 4301.

[18] E. P Giannelis, Advanced Materials. 8 (1996), 29.

[19] S. K Swain, A. I Isayev, Polymer. 48 (2007), 281.

[20] E. Erdmann, F. Monasterio, M. A Toro, H. Dest éfanis, Journal of Materials Science and Engineering A 1. (2011), 778.

[21] C. Lotti, C. S Isaac, M. C Branciforti, R. M. V Alves, S. Liberman, R. E. S Bretas, European

Polymer Journal. 44 (2008), 1346.

[22] P. Neogi, Difussion in polymers. Marcel Dekker Inc. (1996).

[23] G. Choudalakis, A. D Gotsis, European Polymer Journal. 45 (2009), 967.

[24] W. Rabel, Farbe und Lack. 77(10) (1971), 997.